Research Article

Journal of Environmental Nanotechnology

Air Quality Prediction in Smart Environment using Lightweight Residual Network: Sustainable Light-AirNet Approach

P. Muthusamy[1*], V. Nandini[2], B. Karthikeyan[3], K. Nithya[4], S. Sabarunisha Begum[5] and K. Elangovan[6]

[1]Department of Cyber Security, Paavai Engineering College (Autonomous), Namakkal, TN, India
[2]Department of Computer Science and Engineering, Sona College of Technology, Salem, TN, India
[3]Department of Information Technology, Panimalar Engineering College, Chennai, TN, India
[4]Department of CSE, school of computing, Vel Tech Rangarajan Dr. Sagunthala R&D Institute of Science and Technology, Chennai, TN, India
[5]Department of Biotechnology, P.S.R. Engineering College, Sivakasi, TN, India
[6]Department of Mechanical Engineering, Dhanalakshmi Srinivasan University, Perambalur, TN, India
Received: 12.02.2024 Accepted: 19.03.2024 Published: 30.03.2024
*muthu.namakkal@gmail.com

ABSTRACT

In densely populated places, air pollution prediction is crucial since it directly affects human health and the local governance. The main objective of this work is to analyze the spatial and temporal patterns of the concentration of the main air pollutants in Bangalore, India. In this paper, a lightweight residual network with an attention mechanism is created using a collection of residual concatenation blocks layered with recursive residual blocks. This aids in the adaptive extraction of useful features, the learning of more expressive spatial context information, and the efficient transfer of information through gradient flow in the network. A unique attention mechanism, known as the Two-Fold Attention Module, has been created with the purpose of enhancing the model's ability to represent information. The Light-AirNet model was designed to provide hourly forecasts by using past pollution data and three measured weather variables were collected from weather stations. Light-AirNet is compared with existing approaches in terms of different metrics and it was found that it achieves 24.5% of root-mean-square error, 21.5% of mean square error, 12.59% of mean absolute error, and 97.45% of prediction accuracy.

Keywords: Air pollution; Smart environment; Residual network; Spatio-temporal; MSE; MAE; RMSE.

1. INTRODUCTION

People are relocating to cities at an increasing rate, as seen by the rise in the global urban population proportion. The United Nations predicts that 56.15% of the global population will live in urban areas by the year 2025. Then, by 2050, 68% of people on Earth are predicted to reside in urban areas. The issues with air pollution, health care, and logistics are all exacerbated by the expansion of industry and urbanization. Smart cities were developed by combining fixed and mobile sensors with information and communication technology to solve these issues and improve the quality of life of inhabitants. The sensors are positioned across the city to monitor actual human behavior. This idea has developed into a limitless supply of metropolitan data. The regular haze caused by the expansion of industry has resulted in a rapid increase in environmental pollution during the last several decades. Nearly 90% of people breathe air that is polluted and exceeds WHO guidelines for air quality, which can lead to respiratory issues (Ailshire *et al*. 2014; Pöschl *et al.* 2005). Exposure to $PM_{2.5}$, even for short periods ranging from hours to weeks, may increase the probability of cardiovascular disease-related events and fatalities (Du *et al.* 2016). According to the Global Burden of Diseases (Cohen *et al*. 2017; Bu *et al.* 2021), 115.1 million disability-adjusted life years (DALYs) and 4.2 million deaths were attributed to $PM_{2.5}$ exposure in 2015. These figures rose to 142.52 million DALYs and 4.58 million deaths in 2017. In addition to endangering people's health and lives, this poor air quality also poses a threat to the economy. Air pollution may be to blame for 1% of the world's GDP, according to data provided by the Organization for Economic Cooperation and Development. For public health and political decision-making, an efficient system for tracking and monitoring air pollution is essential. However, the mechanism and process of $PM_{2.5}$ formation are very intricate due to the complexity of its features, including its non-linear qualities in time and space (Lu *et al.* 2021), which has a high impact on accuracy and requires special monitoring as a consequence. Air quality forecasting has been widely addressed using conventional statistical methods. The fundamental premise of these approaches is drawing conclusions from past data. The two popular statistical approaches used to predict air quality are ARIMA

(Autoregressive Integrated Moving Average) (Kumar and Jain, 2010) and ARMA (Autoregressive Moving Average) (Bartholomew *et al.* 2017). However, when the amount of data and complexity increases, these methods become less effective due to the length of training process. Machine learning (ML)-based prediction approaches are growing in popularity as big data and AI continue to progress. For using these models, a person does not need understanding of the physical or chemical properties of air pollutants. The most popular ML algorithms are Multiple Linear Regression (MLR), Random Forest (RF) (Yu *et al*. 2016), Support Vector Regression (SVR) (Lin *et al.* 2011), and Artificial Neural Networks (ANN) (Wang *et al.* 2015). These algorithms incorporate complex nonlinear relationships among the concentration of air pollutants and weather variables. The Greater London area's pollution levels have been reliably and accurately measured with an ensemble technique that included numerous ML algorithms (Danesh *et al.* 2020). In order to forecast air pollution across various research regions, many ANN structures have been created, including the neuro-fuzzy NN (Mishra and Goyal, 2016) and the Bayesian neural network (Zaidan *et al.* 2019).

Given this background, the contributions of this work are as follows:

An effective recursive residual block is proposed with a multi-path residual learning approach to improve performance at a minimal computational expense by paying careful attention to spatial-temporal information.

An adaptive rescaling of feature maps is suggested for the attention module to optimize the network's representation power.

2. RELATED WORKS

Deep Learning (DL) is an advancement in ML that makes use of an ANN, which is a multi-layered structure. DL algorithms need minimal human intervention due to automatic extraction of characteristics. However, DL differs significantly from other ML approaches in that it needs a large amount of data to function successfully. Numerous machine learning techniques are available that may be used to address various issues.

Sonawani and Patil (2024) developed a unique method called the gated recurrent unit of multiheaded convolutional neural networks (CNN). This method shows the capacity to predict the pollution concentration for the hour ahead. Additionally, Transfer learning is employed to generate predictions in scenarios involving novel systems with limited data available for prediction. The model achieved an RMSE value of 55.42% when making predictions on a fresh target system with little data. Oliveira *et al.* (2023) used a spatiotemporal graph neural network, which follows the GraphSAGE paradigm, to predict the ozone levels. Jin *et al.* (2023) developed the network which consists of modules that represent spatial and temporal patterns. The spatial module extracts geographic data using GraphSAGE, a graph sampling and aggregation network. In the temporal module, the gated recurrent unit (GRU) is combined with a graph network through the use of a Bayesian (BGraphGRU) to efficiently capture the temporal data. Furthermore, this work utilized Bayesian optimization to address the problem of the model's imprecision. Gilik *et al.* (2022) presented a model which blends a Long short-term memory (LSTM) deep NN with a CNN. This model uses spatial-temporal correlations to predict the air pollution in different parts of a metropolis. Waseem *et al.* (2022) computed the daily and hourly $PM_{2.5}$ concentrations in Pakistan over 30 and 72 hours and evaluated the impact of meteorological circumstances on $PM_{2.5}$ levels. Models such as, LSTM, FbProphet, and LSTM encoder-decoder are examples of DL and ML models that were utilized for the forecasting.

In summary, deep learning struggles with extracting data characteristics in both the spatial and temporal dimensions. The majority of networks fail to comprehensively extract data attributes from both the temporal and spatial aspects. Moreover, a number of models give preference to Euclidean space; nonetheless, the locations of air quality monitoring stations often deviate from ideal circumstances of Euclidean space. Thus, this work presents a novel Lightweight Residual Network with attention mechanism, which effectively addresses the problems of gradient disappearance/explosion in space-time series prediction by utilizing the potential of residual neural networks to capture spatial information and the advantages of attention mechanism.

3. STUDY AREA

Bangalore is located at around latitude 12.97° N and longitude 77.57° E. The whole area of the city is 741 km^2. Being a rapidly expanding metropolis and a significant economic hub, Bangalore often encounters diverse obstacles, including urban expansion, infrastructure requirements, and the effective management of environmental concerns such as air pollution. One of the main reasons for rising levels of Bangalore's air pollution is the city's fast automobile population growth. City is polluted by vehicle emissions from both cars and motorbikes. Congestion is becoming worse and people are still driving older cars without adequate pollution control. Bangalore's rapid development has led to a vast amount of construction activity, which increases particulate matter (PM), aerosol, and dust emissions. The health and environment of Bangaloreans are in danger because of these pollution sources.

3.1 Monitoring Stations

In Bangalore, air quality is monitored by the National Ambient Air Quality Monitoring Program (NAMP). This program is processed by the Central Pollution Control Board (CPCB) in collaboration with the Karnataka state pollution control board (KSPCB). The main aim of the NAMP is to analyze the air quality in various Indian cities and regions. In order to analyze various air pollutants, the project establishes a network of permanent air quality monitoring stations fitted with advanced equipment. These stations are placed to collect the air quality data that fairly depicts different parts of a city. The administration and running of Bangalore's air quality monitoring stations are within the purview of the KSPCB. In Bangalore, there are specific monitoring sites (ST1-ST8) where air quality data is collected and recorded, as specified in Table 1. The existing network of monitoring stations in Bangalore is crucial for comprehending the 231 geographical and temporal variations in air pollution.

Table 1. Monitoring locations in Bangalore city

Code	Station name	Elevation in mm above sea level	Classification of location
ST1	Kadabesanahalli	878	industrial
ST2	Hombegowda Nagar	910	commercial
ST3	Peenya	910	industrial
ST4	BTM	908	commercial
ST5	Bapuji Nagar	853	commercial
ST6	Hebbal	903	industrial
ST7	Silk Board	887	industrial
ST8	Jayanagar	919	commercial

3.2 Data Collection

The monitoring stations are most likely measuring crucial air contaminants. The first phase involves gathering data from the current monitoring stations, which often assess levels of pollutants such as $PM_{2.5}$, PM_{10}, NO_2, SO_2, O_3, and CO. Typically, these stations are strategically positioned in various locations across the city. The air pollution monitoring procedure used in Bangalore includes consistent and methodical data gathering to evaluate the air quality. The monitoring is carried out continuously for a duration of one hour, using varying sample frequency for gaseous pollutants and particulate matter. Air pollution monitoring is conducted biweekly. This regularity enables a systematic and frequent evaluation of air quality conditions throughout the city. The 4-hourly sampling of gaseous pollutants and 8-hourly sampling allow the detection of short-term changes in pollutant levels, including variations that occur at various times of the day.

3.3 Data Preparation

The data collected from the monitoring stations comprises a series of observed values $\{x_t\}$ that are recorded at defined time intervals t. The time series data is taken at hourly intervals. Following the data imputation, we continue to standardize all the observations inside the interval [0,1] using the following method:

$$X_t = \frac{x_t - \min(x_t)}{max(x_t) - \min(x_t)} \quad \ldots (1)$$

Furthermore, the time series is broken down into its trend, seasonality, and irregular components using an additive model (the cyclic component is not included in this study):

$$X_t = trend_t + cyclic_t + seasonal_t + irregular_t \quad \ldots (2)$$

The trend component $trend_t$ at time t represents the long-term evolution of the series, which may be either linear or non-linear. The seasonal component at time t, denoted as $seasonal_t$, represents the fluctuations that occur due to seasonal variation. The irregular component $irregular_t$ (also known as "noise") at time t represents the stochastic and erratic influences. Occasionally, the time series exhibits a cyclic component $cyclic_t$ that represents the recurring but irregular fluctuations.

3.4 Light-AirNet Structure

The Light-AirNet model has many modules, namely the Residual Module which contains a recursive residual block, and the Feature Module which incorporates an Attention Mechanism, as seen in Fig. 1.

Let us designate $\{I_{LR}, I_{SR}\}$ as the input and output of the network. The process begins with a convolutional layer using a kernel size of 3 × 3, which may be expressed as follows:

$$H_{convlayer} = f_{convlayer}(I_{LR}, W_c) \quad \ldots (3)$$

where $f_{convlayer}(.)$ and W_c represent the convolution operation and parameters applied to the input I_{LR}. The term "$H_{convlayer}$" represents the resulting output, which is then used as the input for the Residual Module. Let $H_{rm}^{i,j}$ represent the output of the i-th Residual Concatenation Block (RCB) including the j-th inner recursive residual block (RRB). The Residual Module is a component that may be precisely specified as:

$$H_{RM} = f([H_{convlayer}, \ldots, H_{RCB}^{i-1}(H_{RRB}^{j-1}; W_c^{\,j}), H_{RCB}^{i}]W_c^{i} \quad \ldots (4)$$

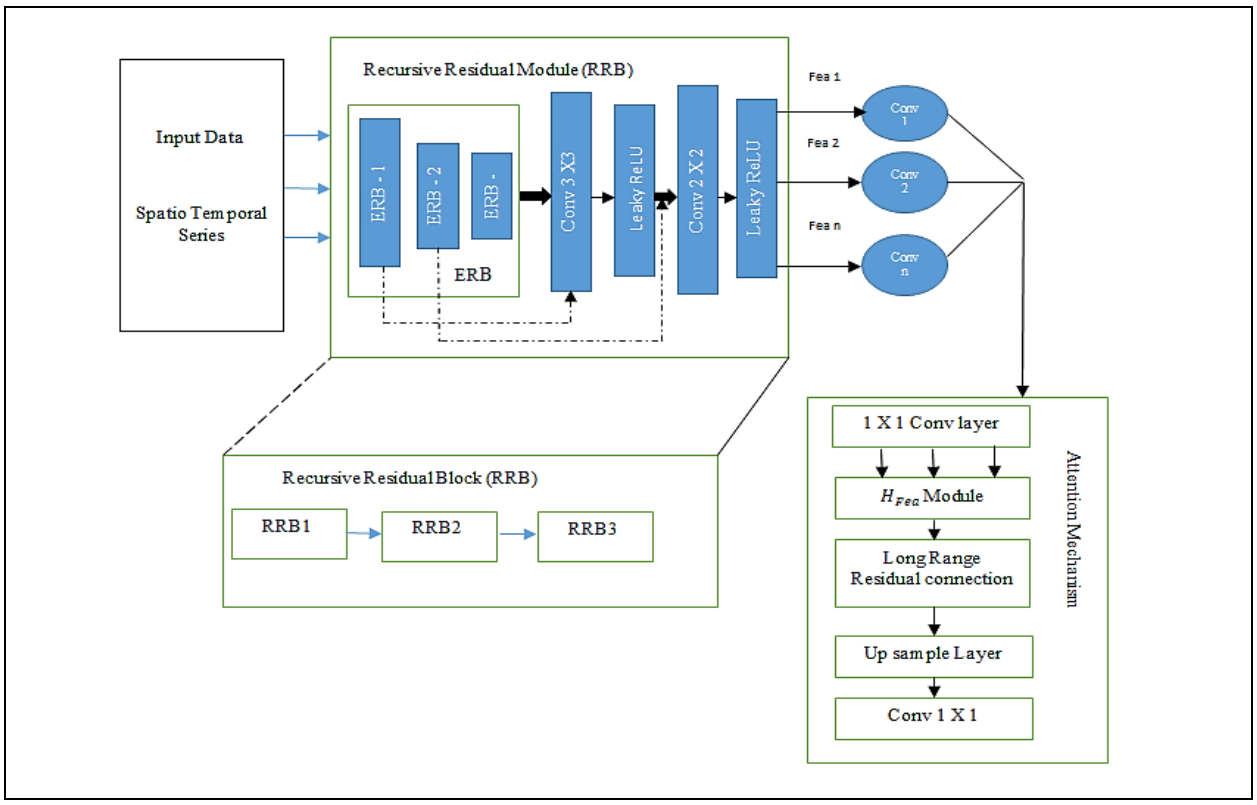

Fig. 1: Overall network architecture of the proposed Light-AirNet

where H_{RM} refers the Residual Module output. It is important to observe that our RM incorporates multiple layers of learning connections, which are then followed by a 1 × 1 convolutional layer. This convolutional layer serves to regulate the output after each block, enabling our model to efficiently transmit information throughout the entire network (from lower to higher layers and vice versa during backpropagation). Additionally, this architecture allows the network to acquire multi-level representations. The i-th RCB may be defined as follows:

$$H_{RCB}^{i} = f([H_{RRB}^{j,R}, \ldots H_{RRB}^{j-1,R}(H^{i-1}; W_c^{i}]); W_c^{j} \quad \ldots (5)$$

Subsequently, the output is sent to the Feature Module where the feature maps are first refined, i.e., recalibrated, inside the module, followed by the extraction of more abstract features. Then , the preceding data are combined to effectively mitigate the issues of gradient vanishing/exploding and ensure that the network may access unaltered information.

$$H_{Fea\_module} = f_{GLOBAL_{FEAT}}(H_{att_{mech}}(H_{res_{mod}}; W_c); W_c) + H_{long\_res} \quad \ldots (6)$$

In this context, $H_{att_{mech}}$ represents the enhanced attention layer, whereas H_{long_res} refers to the LongRange Residual Connection. The last phase involves the use of the MultiScale Module to rebuild the picture using the acquired feature-maps. The convolutional layer immediately follows the upsampling module:

$$H_{up} = f_{pix}(H_{Fea\_module}) \quad (7)$$

where, $f_{pix}(.)$ represents the module function, while H_{Fea_module} denotes the output of the Fea_module. The characteristics that have been increased in size are restored using the convolutional layer.

$$I_{SR} = f_{rec}(H_{up}) = H_{\text{Light-AirNet}}(I_{LR}) \quad (8)$$

where, $f_{rec}(.)$ and $H_{\text{Light-AirNet}}(.)$ refer to the reconstruction layer and function of our Light-AirNet model, respectively.

3.4.1 Enhanced Residual Block (ERB)

The ERB is constructed based on the residual block, aiming to maintain the simplicity of our Light-AirNet model while enhancing its performance. This may be achieved by fully using the multi-layer feature maps inside the ERB. In order to achieve this objective, ERB enhances the input feature $fea_{in} \in R^{H\times W\times C}$ by the use of a 3×3 convolution layer and a LeakyReLU activation function. The feature extracted, represented as $fea_1 \in R^{H\times W\times C/2}$, undergoes further refinement in ERB using a 2 × 2 convolution layer. This refinement process results in the output feature $fea_2 \in R^{H\times W\times C}$.

$$fea_1 = \text{LeakyReLU}(conv_{3\times3}(fea_{in})) \quad \ldots (9)$$

$$fea_2 = conv_{3\times3}(fea_1) \quad \ldots (10)$$

This ERB incorporates a skip connection and a 1×1 convolution to merge the input features (fea_{in} and fea_2) and generates the fused feature (fea_{fuse}):

$$fea_{fuse} = conv_{1\times1}(fea_{in} + fea_2) \quad \ldots (11)$$

Ultimately, this ERB explicitly combines the intermediate feature fea_1 with the fusion feature fea_{fuse} to generate the output feature fea_{out} in the following manner:

$$fea_{out} = conv_{1\times1}(concat(fea_{fuse}, fea_1) \quad \ldots (12)$$

This ERB effectively collects and exploits multi-layer information that correspond to spatially adaptable brightness zones, in contrast to the original residual block. The developed ERB, achieved by making a simple adjustment to the residual block, functions as a lightweight component in the Light-AirNet architecture.

4. RESULTS AND DISCUSSION

This proposed model was trained using an Nvidia Geforce 2080 GPU, which has a memory capacity of 8 GB. The experiment included conducting tests using either 5% or 10% of the data for both validation and testing purposes, while the remaining data was utilized for training. The overall data utilization in the validation and testing phase declined from 10% to 5% for the eight air quality monitoring sites in Bangalore. The processing system used in this investigation comprises a PC fitted with an Intel Core i3 CPU and 8 GB of RAM. The programming language used in this particular scenario for the aims of classification and enhancement is Python 3.9.7.

4.1 Performance Metrics

The performance of the proposed method is evaluated by four metrics. They are coefficient of determination (R^2), mean square error (MSE), mean absolute error (MAE), and root-mean-square error (RMSE). The expressions are:

$$RMSE = \sqrt{\frac{1}{N}\sum_{i=1}^{N}(y'_t - y_t)^2} \quad \ldots (13)$$

$$MSE = \frac{1}{N}\sum_{i=1}^{N}(y'_t - y_t)^2 \quad \ldots (14)$$

$$MAE = \frac{1}{N}\sum_{i=1}^{N}|(y'_t - y_t)^2| \quad \ldots (15)$$

$$R^2 = 1 - \frac{\sum_i^N (y'_t - y_t)^2}{\sum_{i=1}^{N}(y''_t - y_t)^2} \quad \ldots (16),$$

where N denotes the overall quantity of samples in the dataset, y_t and y' symbolize the true value and the average true value of $PM_{2.5}$, whereas y'' represents the projected value of the $PM_{2.5}$ concentration acquired by the model. A decreased number for RMSE, MSE, and MAE indicates a superior prediction ability of the model. For R^2, a score closer to 1 indicates a higher level of accuracy in the model's predictions.

4.2 Comparative Analysis

The comparative analysis is conducted for the existing techniques such as multiheaded convolutional neural networks (MCNN) (Sonawani and Patil, 2024), convolutional neural network and a long short-term memory (CNN+LSTM) (Gilik *et al*. 2022) and the proposed Light AirNet.

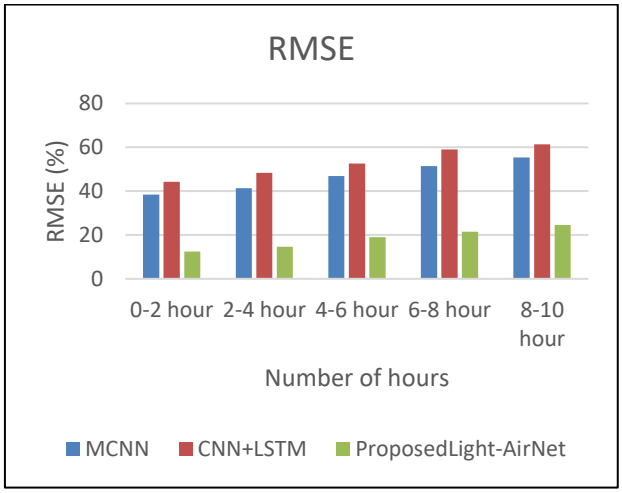

Fig. 2: comparison of RMSE

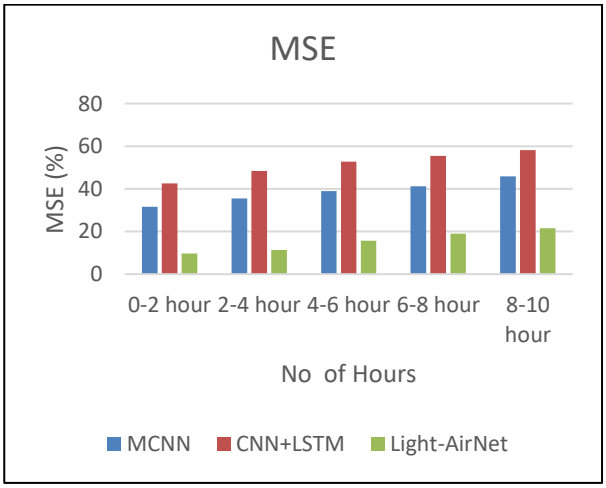

Fig. 3: Comparison of MSE

Figure 2 depicts the comparison of RMSE. The exiting method MCNN has RMSE of 55.42%, and

CNN+LSTM, with an RMSE of 61.4%, correspondingly. Additionally, due to the presence of residual block, the proposed Light-AirNet model achieved the lowest RMSE at 24.5%, showing the effective performance when compared to the other methods.

Figure 3 depicts the comparison of MSE. The exiting method MCNN has MSE of 45.85%, and CNN+LSTM, with an MSE of 58.5%, correspondingly. Due to the presence of residual block, the proposed Light-AirNet model achieved the lowest MSE at 21.5%, showing an effective performance when compared to the other methods.

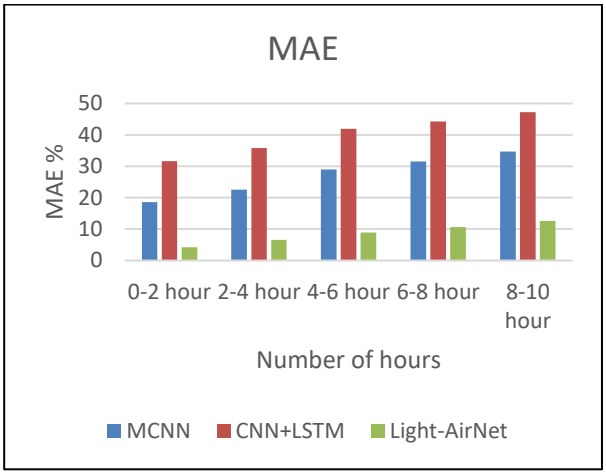

Fig. 4: Comparison of MAE

Figure 4 shows the comparison of MAE, where x-axis shows the hours and y axis shows the MAE (%). The performance of the existing method MCNN and CNN+LSTM achieved 34.68% and 47.2% respectively, whereas the Light-AirNet model achieved 12.59% of MAE, which is the lowest error value.

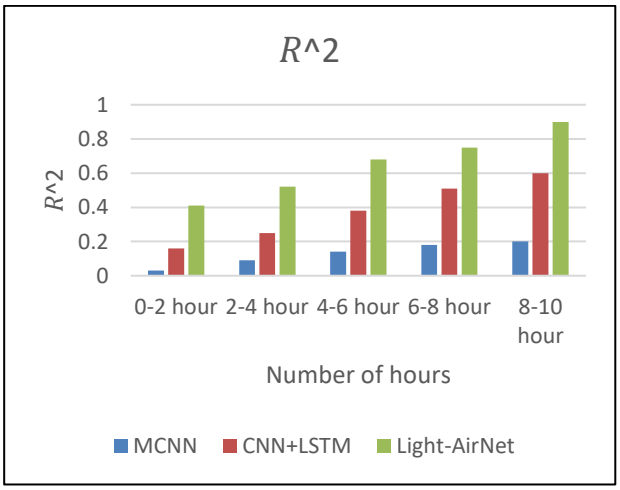

Fig. 5: comparison of R^2

Figure 5 shows the performance of R^2 among the existing method MCNN, CNN+LSTM and the proposed method Light-AirNet. At 8-10 hours, the existing method MCNN and CNN+LSTM achieved 0.2% and 0.6% of R^2, respectively. The proposed Light-AirNet model achieved 0.9% of R^2, the highest value when compared to other methods. Hence, the proposed method demonstrates effective performance.

Table 2 shows the overall comparative analysis of existing methods and proposed methods.

Table 2. Overall comparative analysis

Parameters	MCNN (Sonawani and Patil, 2024)	CNN+LSTM (Gilik *et al.* 2022)	Light-AirNet [proposed]
RMSE (%)	55.42	61.4	24.5
MSE (%)	45.85	58.1	21.5
MAE (%)	34.68	47.2	12.59
R^2 (%)	0.2	0.6	0.9
Prediction accuracy (%)	89.2	79.3	97.45

The comparative study was conducted using the aforementioned parameters with techniques such as multiheaded convolutional neural networks (MCNN) (Gilik *et al.* 2022), convolutional neural network and a long short-term memory (CNN+LSTM) (Gilik *et al.* 2022). However, in relation to work (Gilik *et al.* 2022), the coefficient of determination R^2 is used to assess the accuracy of the modeled values, which are superior than those in (Gilik *et al.* 2022). Nevertheless, Light-AirNet model still outperforms in terms of RMSE and R^2. When comparing the findings of this work with several deep learning methods analysed in literature (Gilik *et al.* 2022; Waseem *et al.* 2022; Jin *et al.* 2023), it is evident that the attention enhanced model consistently showed comparable or better performance. In a recent study (Gilik *et al.* 2022), Light-AirNet demonstrated its ability to accurately represent the spatiotemporal relationships involved in ozone modeling. It significantly improved ozone prediction by 97.45% compared to the reference model (Gilik *et al.* 2022) across several seasons.

5. CONCLUSION

The air pollution in Bangalore city was predicted by employing neural network in a geo-spatial environment. This resulted in development of pollution dispersion maps for the principal gas pollutants. This work introduces a Light-AirNet model with an attention mechanism to accurately estimate the concentration of $PM_{2.5}$ by considering both the temporal and geographical dimensions of air quality data. The mixed network model employs a recursive residual module as the first step to extract spatial dimension information from the data. This model effectively captures and analyzes the attributes of the data in both temporal and spatial dimensions,

addressing typical gradient issues in time series prediction to enhance prediction precision. The minimal cost of this model makes it simple to implement in other networks. This architecture benefits from both propagating information around the network and multi-level learning connections.

In further studies, we will evaluate the developed model using a more intricate time series dataset and attempt to further enhance the overall prediction performance of the model by combining the graph neural network with other optimization techniques and their variations.

FUNDING

This research received no specific grant from any funding agency in the public, commercial, or not-for-profit sectors.

CONFLICTS OF INTEREST

The authors declare that there is no conflict of interest.

COPYRIGHT

REFERENCES

Ailshire, J. A., Crimmins, E. M., Fine particulate matter air pollution and cognitive function among older US adults, *Am. J. Epidemiol*., 180(4), 359–66 (2014). https://doi.org/10.1093/aje/kwu155

Bartholomew, D. J., Time series analysis forecasting and control, *J. Oper. Res. Soc*., 22(2), 199–201 (2017). https://doi.org/10.1057/jors.1971.52

Bu, X., Xie, Z., Liu, J., Wei, L., Wang, X., Chen, M. and Ren, H., Global pm2.5-attributable health burden from,. to 2017: estimates from the global burden of disease study 2017, *Environ Res.*, 197, 1-9 (2021). https://doi.org/10.1016/j.envres.2021.111123

Danesh, Y. M., Kuang, Z., Dimakopoulou, K., Barratt, B., Suel, E., Amini, H., Lyapustin, A., Katsouyanni, K., Schwartz, J., Predicting fne particulate matter (pm2. 5) in the greater London area: an ensemble approach using machine learning methods, *Remote Sens*., 12(6), 1-18 (2020). https://doi.org/10.3390/rs12060914

Cohen, A. J., Brauer, M., Burnett, R., Anderson, H. R., Frostad, J., Estep, K., Balakrishnan, K., Brunekreef, B., Dandona, L., Dandona, R., Feigin, V., Freedman, G., Hubbell, B., Jobling, A., Kan, H., Knibbs, L., Liu, Y., Martin, R., Morawska, L., Pope, C. A., Shin, H., Straif, K., Shaddick, G., Thomas, M., Dingenen, R., Donkelaar, A., Vos, T., Murray, C. J. L., Forouzanfar, M. H., Estimates and 25-year trends of the global burden of disease attributable to ambient air pollution: an analysis of data from the global burden of diseases study 2015, *Lancet*.,389(10082), 1907–1918 (2017). https://doi.org/10.1016%2FS0140-6736(17)30505-6

Du. Y., Xu, X., Chu, M., Guo, Y. and Wang, J., Air particulate matter and cardiovascular disease: the epidemiological, biomedical and clinical evidence, *J. Thoracic. Dis*., 8(1), E8-E19 (2016). https://doi.org/10.3978/j.issn.2072-1439.2015.11.37

Gilik, A., Ogrenci, A. S. and Ozmen, A., Air quality prediction using CNN+ LSTM-based hybrid deep learning architecture, *Environ. Sci. Pollut. Res.*, 29(8), 11920-11938 (2022). https://doi.org/10.1007/s11356-021-16227-w

Jin, X. B., Wang, Z. Y., Kong, J. L., Bai, Y. T., Su, T. L., Ma, H. J. and Chakrabarti, P., Deep spatio-temporal graph network with self-optimization for air quality prediction. *Entropy*, *25*(2), 1-15 (2023). https://doi.org/10.3390/e25020247

Kumar, U. and Jain, V., Arima forecasting of ambient air pollutants (O3, NO, NO2 and CO), *Stochastic Environ. Res. Risk Assess.*, 24(5), 751–60 (2010). https://doi.org/10.1007/s00477-009-0361-8

Lin, K. P., Pai, P. F. and Yang, S. L., Forecasting concentrations of air pollutants by logarithm support vector regression with immune algorithms, *Appl. Math. Comput.*, 217(12), 5318–5327 (2011). http://dx.doi.org/10.1016/j.amc.2010.11.055

Lu, D., Mao, W., Xiao, W., Zhang, L., Non-linear response of pm2.5 pollution to land use change in China, *Remote Sens.*, 13(9), 1-13 (2021). https://doi.org/10.3390/rs13091612

Mishra, D. and Goyal, P., Neuro-fuzzy approach to forecasting ozone episodes over the urban area of Delhi, India, *Environ Technol Innov.*, 5, 83–94 (2016). https://doi.org/10.1016/j.eti.2016.01.001

Oliveira, S. V., Costa, R. P. A., Scott, J., Van, G. Thé, J. and Gharabaghi, B., Spatiotemporal air pollution forecasting in houston-TX: a case study for ozone using deep graph neural networks, *Atmos.*, *14*(2), 1-23 (2023). https://doi.org/10.3390/atmos14020308

Pöschl, U., Atmospheric aerosols: composition, transformation, climate and health effects, *Angew. Chem. Int. Ed*., 44(46), 7520-7540 (2005). https://doi.org/10.1002/anie.200501122

Sonawani, S. and Patil, K., Air quality measurement, prediction and warning using transfer learning based IOT system for ambient assisted living, *Int. J. Pervasive Comput. Commun.*, *20*(1), 38-55 (2024). https://doi.org/10.1108/IJPCC-07-2022-0271

Wang, P., Liu, Y., Qin, Z., Zhang, G., A novel hybrid forecasting model for pm10 and so2 daily concentrations, *Sci. Tot. Environ*., 505,1202–1212 (2015). https://doi.org/10.1016/j.scitotenv.2014.10.078

Waseem, K. H., Mushtaq, H., Abid, F., Abu-Mahfouz, A. M., Shaikh, A., Turan, M. and Rasheed, J., Forecasting of air quality using an optimized recurrent neural network, *Processes*, *10*(10), 1-20 (2022). https://doi.org/10.3390/pr10102117

Yu, R., Yang, Y., Yang, L., Han, G. and Move, O. A., RAQ-A random forest approach for predicting air quality in urban sensing systems, *Sensors*, 16(1), 1-18 (2016). https://doi.org/10.3390/s16010086

Zaidan, M. A., Dada, L., Alghamdi, M. A., Al-Jeelani, H., Lihavainen, H., Hyvärinen, A. and Hussein, T., Mutual information input selector and probabilistic machine learning utilisation for air pollution proxies, *Appl. Sci.*, 9(20), 1-20 (2019). https://doi.org/10.3390/app9204475